IntechOpen

Perspective Chapter:

Intelligent Adaptive Flight Control Augmentation of a Dynamic Inversion Autopilot

Quang M. Lam[1] and Anthony J. Calise[2]
JESPLSOFT Corp, Fairfax, VA 22030

Nhan T. Nguyen[3]
NASA Ames Research Center, Moffett Field, CA 94035

Abstract

High speed UAV flight control is challenged by unknown external aerodynamic disturbances and internal system variations due to complex aerodynamic configuration, propellant consumption, center of gravity movement and possible actuators failures. Redundant aerodynamic control effectors and engine inlet control mechanisms are exploited/blended to maintain adequate force/moment control to satisfy flight control reliability requirements. A control allocation (CA) mixing matrix is an essential element of the redundancy design in addressing fault tolerance capabilities. This paper employs an Intelligent Flight Controller (IFC) implemented in an adaptive control augmentation fashion to assist the UAV's primary Nonlinear Dynamic Inversion (NDI) controller in restoring aircraft stability and command following objective when subjected to effector performance degradation, including failures. Through a blended design between Optimal Control Modification (OCM) and Derivative-Free Model Reference Adaptive Control (DF-MRAC), the IFC offers a performance consistency in comparison to traditional MRAC. The proposed IFC framework has demonstrated its effectiveness in assisting the baseline NDI flight control system to maintain its mission subjected to actuators failures (via an implicit automatic CA 're-distributing' action.) Furthermore, the IFC also works well with any existing onboard CA algorithm in dealing with effector failures, without requiring restructuring of the CA blending matrix. It therefore deserves consideration for application to future high Mach UAVs.

Keywords: Nonlinear Dynamic Inversion (NDI), Control Allocation (CA), Optimal Control Modification (OCM), Derivative Free Model Reference Adaptive Control (DF-MRAC), Direct Adaptive Control (DAC), Passive CA, Fault Tolerant Control (FTC)

[1] CTO, Ph. D., Quang.Lam@Jesplsoft.com
[2] Board's Advisor & Chief Technologist, Ph. D., Anthony.Calise@Jesplsoft.com
[3] GNC Group Lead, Ph. D., Nhan.T.Nguyen@NASA.gov

1. Introduction

Flight Control Systems (FCSs) are one of the most important safety critical systems in modern aircraft and high-speed UAVs. Redundancy of both FCS software (FSW) and its associated actuators/effectors (aerodynamic control surfaces and engine inlet control mechanisms) are exploited to achieve robust performance and high reliability against component failures (*hardware and/or software redundancy, e.g.,* see [1-2]). For hardware redundancy, multiple control effectors are designed and sized to adequately produce 6 Degree-of-Freedom (DOF) Force/Moment (F/M) responses in order to closely follow the commanded F/M profiles generated by the control law (CLAW) so that the aircraft can maintain its maneuvering ability subject to one or more effector failures. For example, with loss of one elevon and one canard out of a total of 7 aerodynamic control surfaces, the aircraft may still be able to maintain its 6DOF controllability.

This paper investigates the employment of the intelligent flight control (IFC) architecture developed in [4] for a Generic Transport Model (GTM) aircraft, and further adopts, modifies, and implements the IFC in a control augmentation fashion to assist the Aerodynamic Model in Research Environment (ADMIRE) fighter aircraft FCS [5] in effectively maintaining its 6DOF FCS performance when subjected to two stuck inner elevons. It is shown that with the baseline dual loop NDI-FCS alone the aircraft fails to maintain its desired flight mission and consequently its flight profile is pre-maturely terminated. The investigation studies herein also uncover several key connections or findings between adaptive control (CLAW side of FSW) and adaptive control allocation. One key connection between CLAW and CA is that the adaptive signal generated by the IFC is effective on the CLAW side in improving command tracking while at the same time improving CA actions in assigning which effectors should be utilized to achieve the required NDI F/M commands. Sections 2 and 5 of this paper will present these interesting details, while Sections 3 and 4 describe the problem statement of the baseline NDI controller subject to 2 stuck elevons and present the IFC formulation, respectively.

2. ADMIRE Baseline Controller Description

The ADMIRE fighter jet and its development of a Generic Flight Controller are presented in detail in [6] and [8]. However, for completeness it is briefly described here so its baseline FCS interface with the IFC block added in an adaptive control configuration can be accurately described and presented. The ADMIRE's generic dual loop design flight controller is employed in this study wherein the outer loop (i.e., slow dynamic loop) is designed to be command following. This amounts to achieving the angle of attack (AoA) command following for the longitudinal channel and for the angle of sideslip (AoS) and stability axis roll rate command following for the lateral and directional channels. The pitch/roll stick and rudder pedal commands are appropriately shaped and scaled to result in the AoA, stability axis roll rate and AoS commands. A block schematic of the generic flight controller is shown in Figure 1. The inner loop (or fast dynamic loop) is designed using the Nonlinear Dynamic Inversion (NDI) adopted from [6] and detailed in the Appendix Section of the book for ADMIRE integration. The controller structure has the outer

loop regulation of the slow dynamics consisting of the AoA, AoS, and flight path angle (FPA) by commanding the inner loop angular rates.

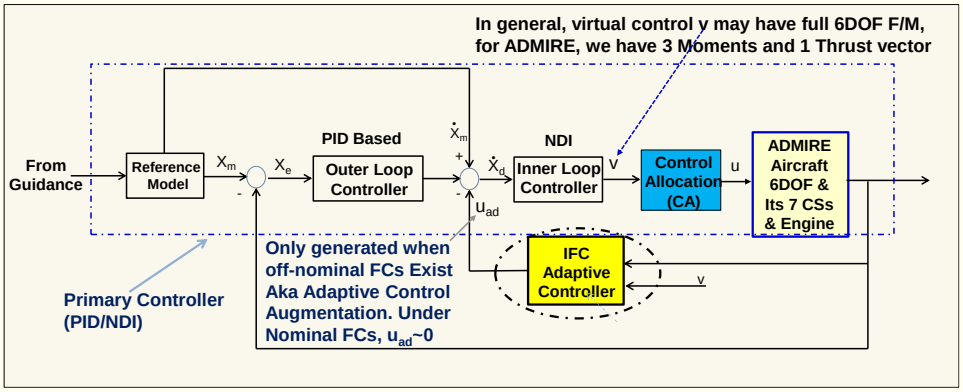

Figure 1: ADMIRE Dual Loop Autopilot with IFC Implementation in an Augmentation Fashion – Baseline PID/NDI Not Using Full State Feedback.

ADMIRE has seven aerodynamic control surfaces (CSs): left and right canards, left and right in-board elevons, left and right out-board elevons, and 1 rudder (see Figure 2.) The canards and elevons can be operated together or in symmetric or differential deflections or individually. The roll, pitch, and yaw channels are controlled using these control surfaces. Hence, the transformation matrix has dimension 7 by 3 (3 desired control moments transformed to 7 CS deflections). The dual loop PID/NDI autopilot is detailed in [7] for readers who are interested in seeing how the commanded state vectors of both the outer loop and inner loops are being formulated. This paper is intended to focus on the IFC algorithm description and how it differs from [4] in the implementation. Note that the current ADMIRE simulation has a single engine; however, the engine throttle controller has not been jointly integrated with the 7 CSs main PID/NDI controller. Nonetheless, it is being accounted for in the existing 7 CA algorithms block (see Figure 3 below and [6] for algorithm details) to jointly map 'virtual' Force/Moment (F/M) command to 'real' effectors. For future UAVs missions, especially for high performance UAVs with flight speeds beyond Mach 5, a high dimension effectors vector including advanced engine control effectors can be defined to address a more effective mixing scheme.

For the purposes of the roll axis control (the first column of $\boldsymbol{B}_{v2r}$ matrix, *virtual to real (v2r)*) the differential canards (KR2) and differential elevons (KR4) are used. For the pitch axis control (2nd column of $\boldsymbol{B}_{v2r}$ matrix the symmetric canards (KP1) and symmetric elevons (KP3) are used (see [6] & [8] for background). Finally for the yaw axis control (3rd column of B matrix,) the differential canards (KY2), differential elevons (KY4) and rudder (KY5) are used. The control allocation matrix is given by:

$$\boldsymbol{B}_{v2r} = \begin{bmatrix} -\boldsymbol{KR}_2 & \boldsymbol{KP}_1 & -\boldsymbol{KY}_2 \\ \boldsymbol{KR}_2 & \boldsymbol{KP}_1 & \boldsymbol{KY}_2 \\ -\boldsymbol{KR}_4 & \boldsymbol{KP}_3 & -\boldsymbol{KY}_4 \\ -\boldsymbol{KR}_4 & \boldsymbol{KP}_3 & -\boldsymbol{KY}_4 \\ \boldsymbol{KR}_4 & \boldsymbol{KP}_3 & \boldsymbol{KY}_4 \\ \boldsymbol{KR}_4 & \boldsymbol{KP}_3 & \boldsymbol{KY}_4 \\ \boldsymbol{KR}_5 & \boldsymbol{KP}_5 & \boldsymbol{KY}_5 \end{bmatrix} \quad \textbf{(1)}$$

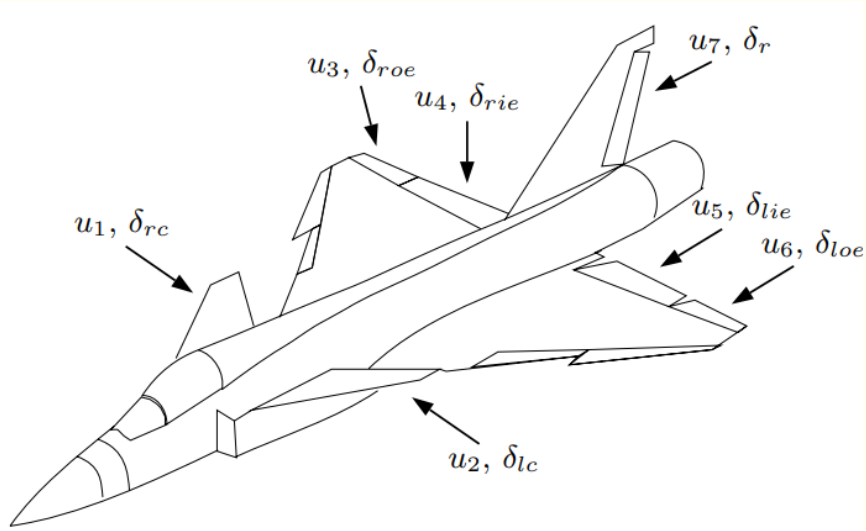

Figure 2: ADMIRE's Seven Aerodynamic Control Surfaces (u_i, i=1,2,...7).

- KR5 is the aileron to rudder interconnect gain. In case the optimizer finds a solution greater in magnitude than 1.2, it is reset to 1.2. The maximum differential deflection of the elevons is 25 degrees, whereas that of the rudders is 30 degrees. Therefore, limiting the KR5 gain to 1.2, prevents a control surface saturation of the rudder due to a roll command at the expense of some sideslip buildup during roll maneuver about the stability axis.
- The maximum roll rate in the stability axis (velocity vector direction) is computed using the control allocation matrix determined above and used for the forward path (body x axis direction) command scaling throughout the airspeed range.

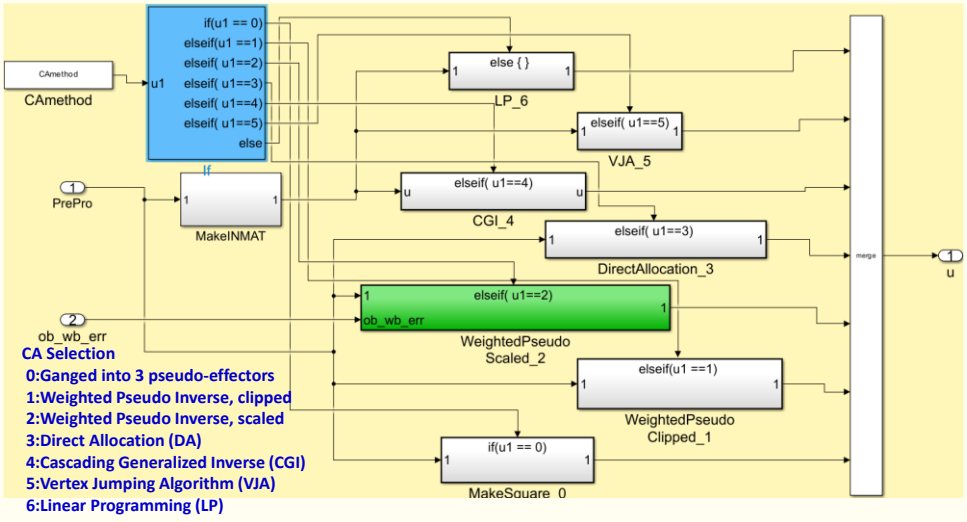

Figure 3: Current ADMIRE CA Block with Existing 7 CA Algorithms & IFC works quite well with any of those 7 without imposing any restructuring CA action.

3. Impact of Two Stuck Inboard Elevons on the Baseline NDI FCS

In addition to the phase and gain margins, the following should be taken into consideration to ensure HQ criteria are met: (1) Effector performance degradation due to wear/tear or unexpected damage due to adversarial actions; (2) effector deflection and rate limits which could destabilize UAV FCS performance (see [10] and [23]); (3) the AoA rate $\dot{\alpha}$ which should be safeguarded and not exceed an upper bound (e.g., <25 deg/s) throughout the flight envelope (with an AoA bound not to exceed 40 deg); (4) full stick maximum roll acceleration 'Limit Bounds' violation; (5) AoS limit during roll maneuvers; (6) model following errors bound violation (e.g., see [23]) . One of the key concepts going forward to satisfy high speed UAV mission requirements is to jointly optimize F/M at the full 6DOF CLAW level as full 6DOF (currently ADMIRE has not met this design goal), to compute the desired F/M demand (whether a completely healthy set of effectors or a reduced set of degraded capacity effectors exists) and to produce a realistic attainable F/M response.

Figures 4a and 4b present the ADMIRE Baseline FCS CS and trajectory performance under nominal operating conditions with 7 healthy CSs (RC: Right Canard, LC: Left Canard, ROE: Right Outboard Elevon, RIE: Right Inboard Elevon, LIE: Left Inboard Elevon, LOE: Left Outboard Elevon, and RUD: Rudder.)

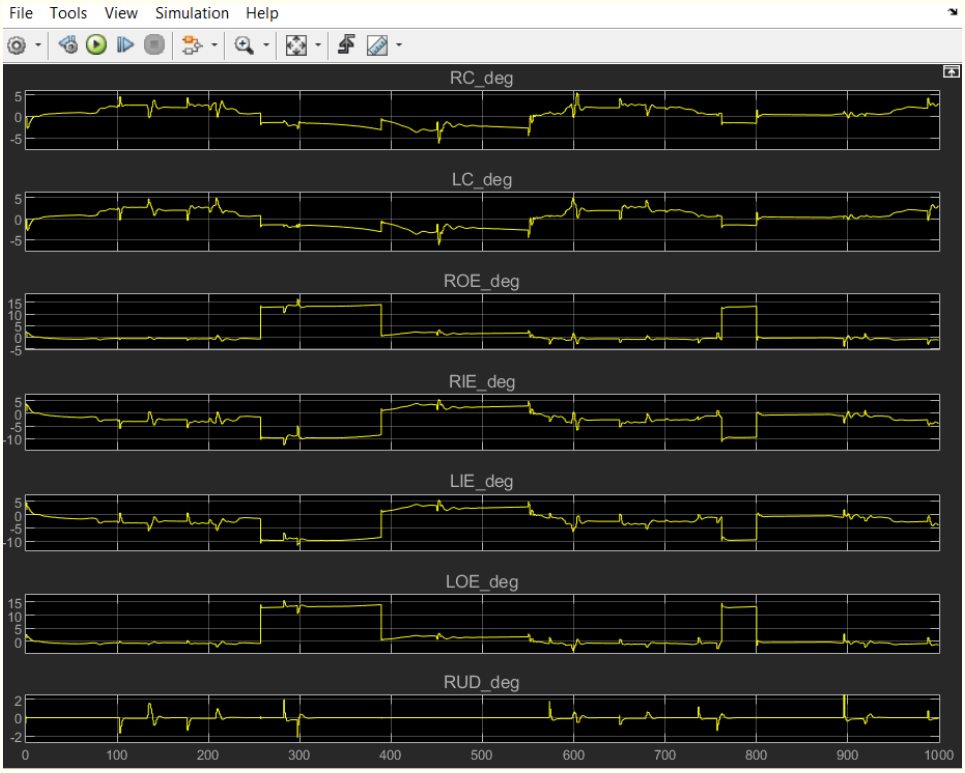

Figure 4a: 7 CSs Deflections Under Nominal FCs.

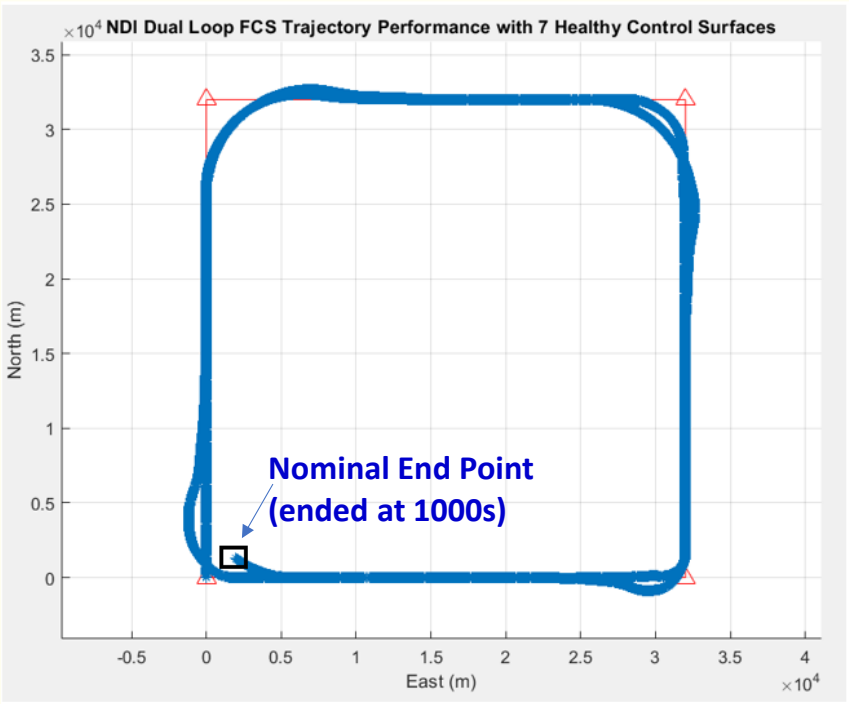

Figure 4b: ADMIRE Nominal Flight Trajectory Performance with 7 Healthy Control Surfaces.

The ADMIRE FCS performance when two inner elevons stuck at and beyond 200 seconds are shown in Figures 5a and 5b. Under this failure the ADMIRE flight trajectory is prematurely terminated at 433 seconds as shown in Figure 5c. The angular acceleration, angular rate, and attitude commands following comparisons are presented in Figures 6 to 8.

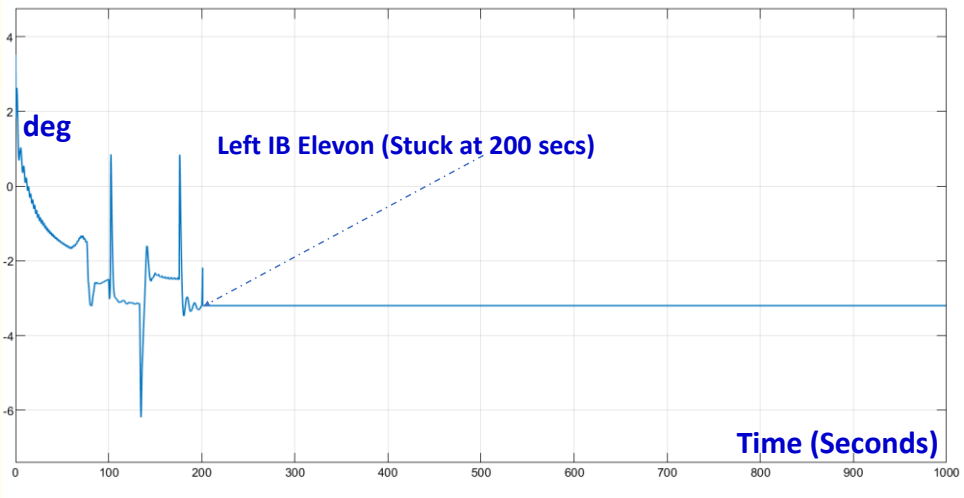

Figure 5a: Left Inboard (IB) Elevon (stuck at 200 seconds.)

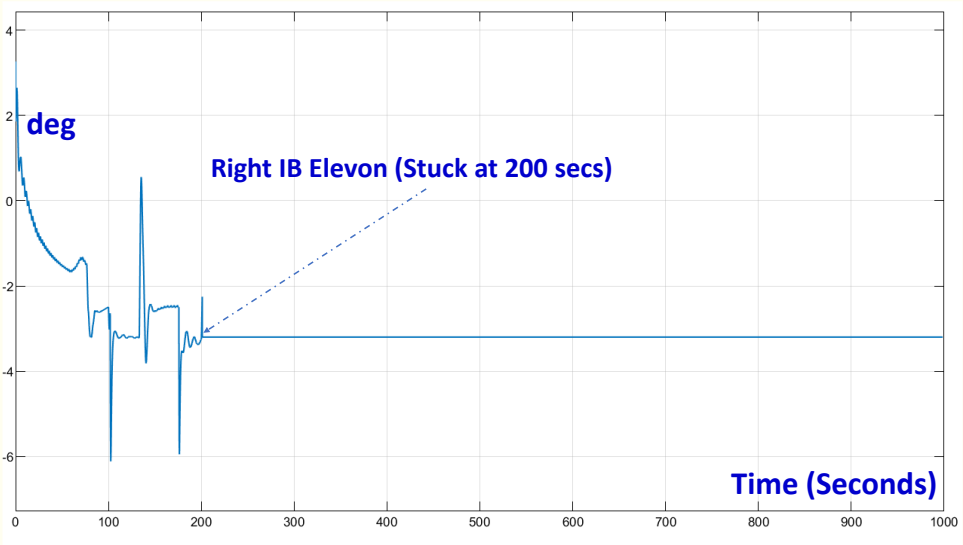

Figure 5b: Right Inboard (IB) Elevon (stuck at 200 seconds.)

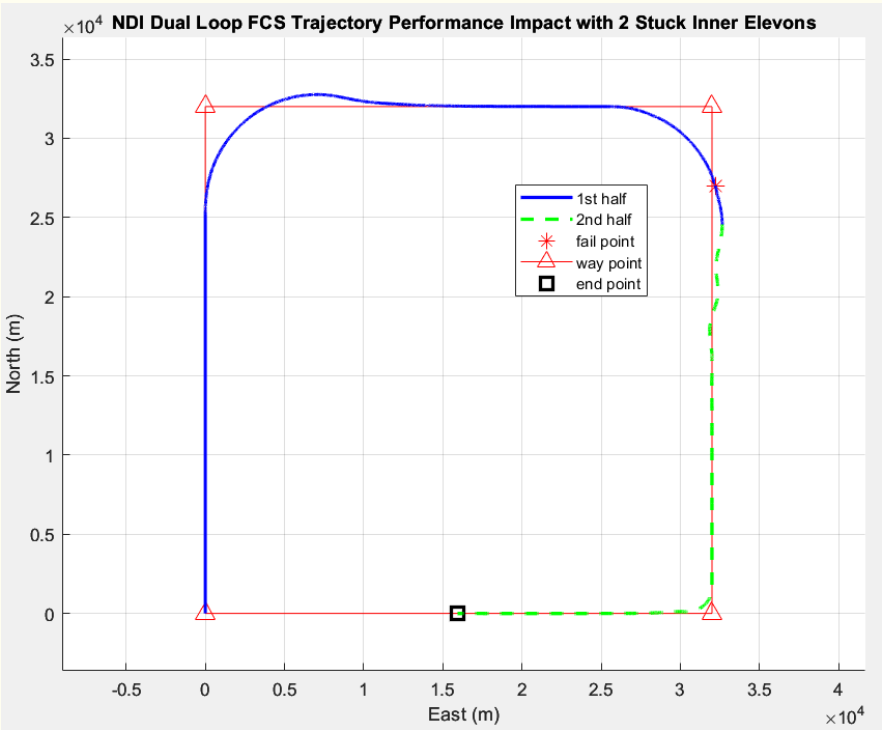

Figure 5c: ADMIRE Flight Trajectory Performance Degradation with Two Stuck IB Elevons (Mission Ended Pre-Maturely with Attitude Pointing Accuracy Severely Degraded).

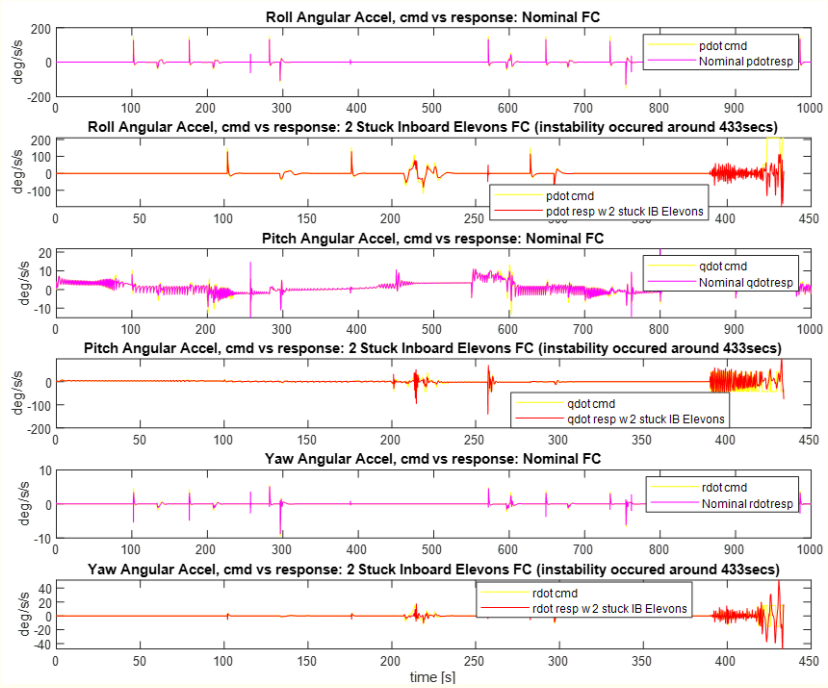

Figure 6: FCS Angular Acceleration Command Following via NDI – Nominal vs 2 Stuck IB Elevons.

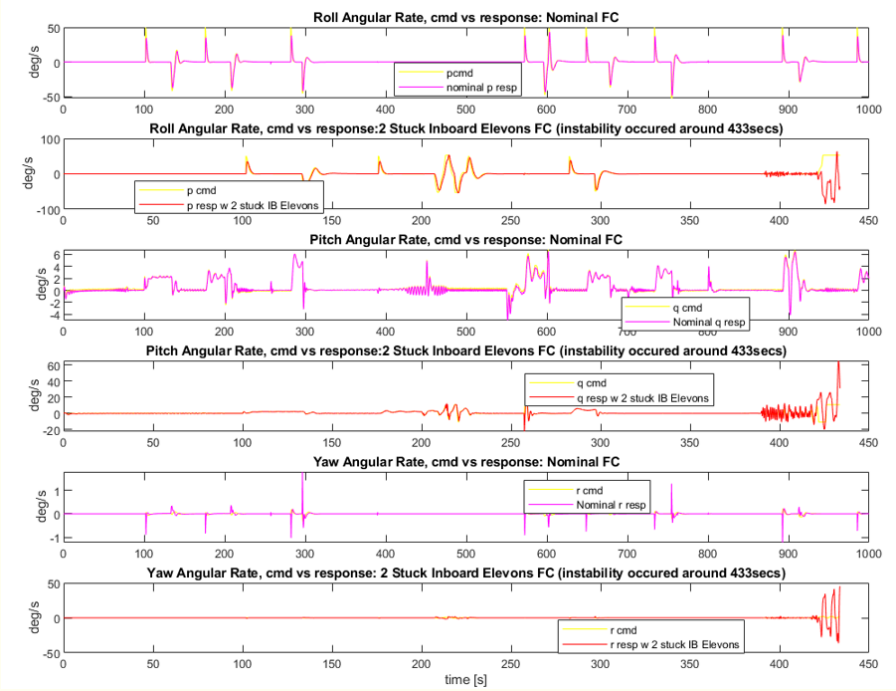

Figure 7: FCS Angular Rate Command Following via NDI – Nominal vs 2 Stuck IB Elevons.

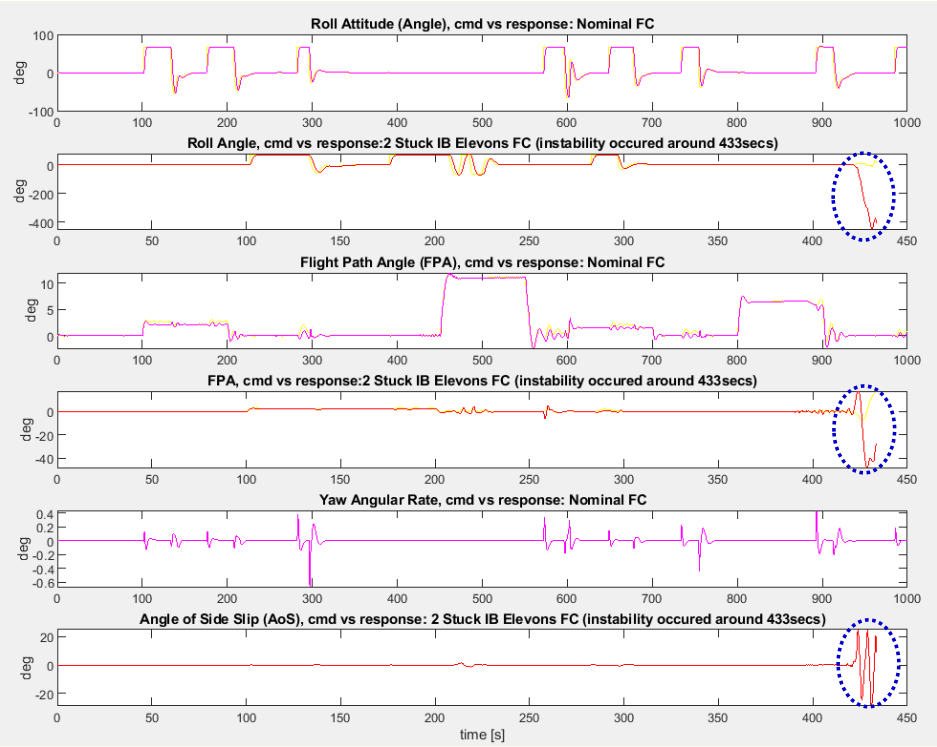

Figure 8: FCS Bank Angle, Flight Path Angle (FPA), and AoS Command Following via NDI – Nominal vs 2 Stuck IB Elevons (causing instability occurred at 433 secs).

These figures demonstrate that with two stuck IB elevons, the ADMIRE fighter aircraft FCS is not able to complete its mission. As a result, modern adaptive control augmentation of some fashion is needed to augment/assist the primary baseline FCS to cope with degraded flight conditions. In Section 4 we describe such an adaptive control augmentation concept using a hybrid adaptive control framework to best assist the primary FCS in completing its missions when subjected to unknown uncertainties and control effector failures.

4. IFC Algorithm Description

IFC algorithms have become popular in improving FCS performance, especially when employing the Optimal Control Modification (OCM) [30] as an adaptive law design modification, to further enhance the controller's ability to cope with unknown uncertainties, aircraft damage, and disturbance attenuation since the early 2000s. We have teamed with NASA Ames Research Center to leverage their work on the IFC development for the NASA GTM piloted simulation [31], and the actual piloted F-15 and F-18 [32] flight tests of the OCM adaptive control law at NASA Armstrong Flight Research Center [4]. Toward this end, we have adopted their GTM-IFC design for robustness enhancement of the ADMIRE FCS when subjected to degraded control surfaces. The IFC block that we adopted from [4] and [12] can be considered a hybrid design as shown in Figure 9. The baseline adaptive control block (shown in yellow) is architected using the direct Model Reference Adaptive Control (MRAC), while the Neural Network Controller (NNC) block offers an

adaptive learning process that allows the NNC-MRAC combination to achieve its adaptation in a more consistent and robust manner.

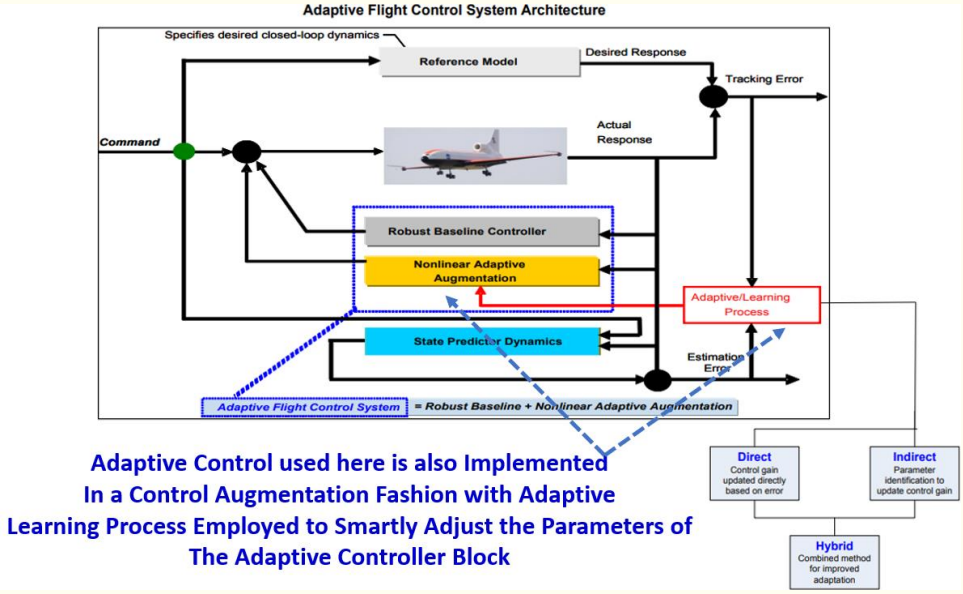

Figure 9: Adaptive Control Motivation for why a Hybrid Design should be Exploited to Achieve Verification and Validation [12].

The IFC architecture developed for GTM [4] that is adopted here is shown in Figure 10. For the ADMIRE FCS performance enhancement subject to imperfect cancellation of the NDI CLAW due to off-nominal flight conditions (i.e., stuck control surfaces and/or completely loss of some control surfaces.) For the sake of describing how the IFC design developed in [4] for aircraft flight control is applied to the ADMIRE's robustness enhancement study, we re-use Section B of [4] (i.e., Neural Network (NN) Direct Adaptive Control) and define its input/output (I/O) for the neural network adaptive control signal, u_{ad}, and how that signal is computed using the ADMIRE aircraft states vector.

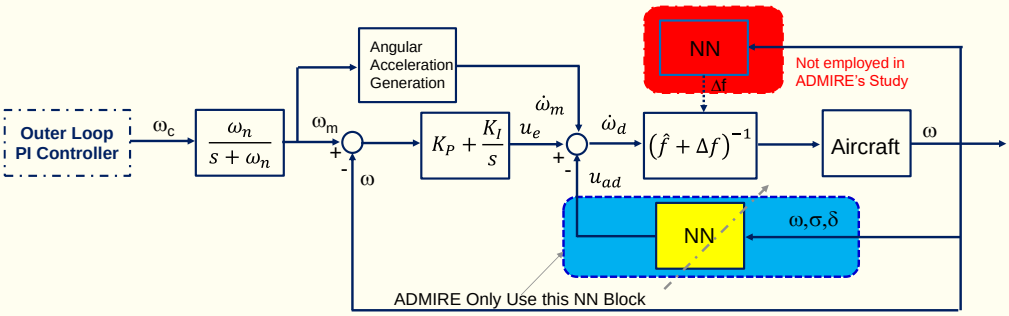

Figure 10: NNC Architecture (Yellow Block) & Their I/O Interface with ADMIRE Aircraft's State Vector.

NN Based Adaptive Control Using Conventional MRAC

The adaptive control augmentation vector u_{ad} is based on the adaptation law by Rysdyk and Calise [11] with a modification to include additional product terms that appear in the nonlinear plant dynamics described by Eqs. (31–33) of [4]:

$$u_{ad} = W^T \beta_{nn}(C_1, C_2, C_3, C_4, C_5, C_6) \quad (2)$$

where β_{nn} is a vector of basis functions computed using Kronecker products with C*i*, *i* =1; . . . ; 6, as inputs into the neural network consisting of control commands, sensor feedback, and bias terms. More specifically, the product terms are

$$C_1 = V^2[\omega^T \quad \alpha\omega^T \quad \beta\omega^T] \quad (3)$$

$$C_2 = V^2[1 \quad \alpha \quad \beta \quad \alpha^2 \quad \beta^2 \quad \alpha \quad \alpha\beta^2] \quad (4)$$

$$C_4 = [p\omega^T \quad q\omega^T \quad r\omega^T] \quad (6)$$

$$C_5 = [u\omega^T \quad v\omega^T \quad w\omega^T] \quad (7)$$

$$C_6 = [1 \quad \theta \quad \phi \quad C_T] \quad (8)$$

The NN basis function, β_{nn}, then expressed as

$$\beta_{nn} = [C_1 \quad C_2 \quad C_3 \quad C_4 \quad C_5 \quad C_6]^T \quad (9)$$

The network weights W are computed by a direct adaptive law, which incorporates a learning rate G > 0 and an e-modification term [12] μ >0 according to the following weight update law

$$\dot{W} = -\Gamma(\beta_{nn} e^T PB + \mu||e^T PB||W) \quad (10)$$

where Γ is an adaptation gain matrix, the matrix P solves the Lyapunov equation $A^T P + P^T A = -Q$ for some positive-definite matrix Q, e is the model following error, and ||.|| is a Frobenius norm. Table 1 shows how P is computed for use in the ADMIRE IFC application. The β_{nn} implementation (of Eq. (9)) is shown in Figure 11.

The e-modification term in Eq. (10) provides a robustness in the adaptive law [14]. The weight update law in Eq. (10) guarantees the stability of the neural network weights and the tracking error. The proof of this update law using the Lyapunov method is provided by Rysdyk and Calise [13].

In the above expressions [α, β, ϕ] are the AoA, AoS, and bank angle, [u v w] are the velocity vector components in the body frame, and ω is the vehicle body frame angular velocity vector.

Table 1: Lyapunov Function Block used in ADMIRE IFC Block.

```
%% See the IFC/NN Based Controller Block
ifc.Kp_p=3; ifc.Kp_q=16; ifc.Kp_r=5;
Ap=-ifc.Kp_p; Bp=ifc.Kp_p; Cp=1; Dp=0;
Aq=-ifc.Kp_q; Bq=ifc.Kp_q; Cq=1; Dq=0;
Ar=-ifc.Kp_r; Br=ifc.Kp_r; Cr=1; Dr=0;
Kp=diag([ifc.Kp_p,ifc.Kp_q,ifc.Kp_r]);
Pmat=lyap(-Kp',eye(3));
Pmat=[  0.1667       0       0
        0       0.0312      0
        0          0     0.1000];
Bmat=eye(3);
```

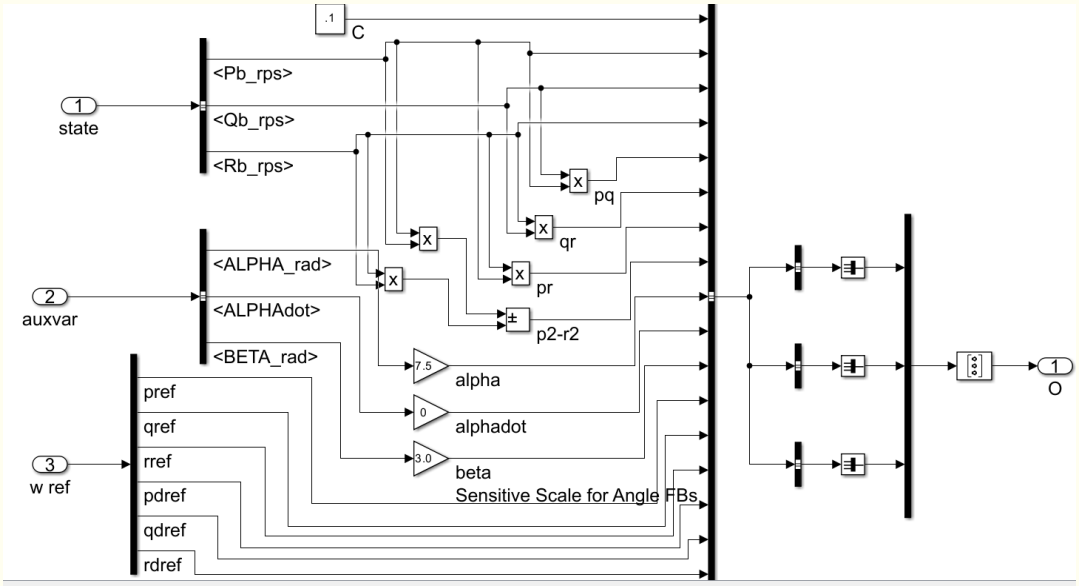

Figure 11: β_{nn} Implementation in ADMIRE FCS IFC Block (not Full State FB.)

3. Derivative Free Model Reference Adaptive Control (DF-MRAC)

The DF-MRAC design framework is fully described in the recently published book written by Yucelen and Calise [9]. Here we just want to describe how it is being used to solve the problem of two stuck in-board elevons by mixing its solution with the IFC architecture described in previous section. The adaptive law in DF-MRAC has the form

$$\widehat{W}(t) = \Omega_1 \widehat{W}(t-\tau) + \widehat{\Omega}_2(t),\ t > \tau \tag{11}$$

where $\tau > 0$, Ω_1 and $\widehat{\Omega}_2(t)$ satisfy:

$$0 \leq \Omega_1^{\mathrm{T}} \Omega_1 < I_s \tag{12}$$

$$\widehat{\Omega}_2(t) = \kappa_2 \beta\big(x(t)\big) e^T(t) P B,\ \ \kappa_2 > 0 \tag{13}$$

There is no need for e-modification as in (10) with this adaptive law and the time delay τ can be freely chosen. DF-MRAC has many other advantages not present in MRAC that are illustrated in [9], including a natural robustness to unmodeled dynamics, greatly improved performance when augmenting a baseline controller that employs proportional + integral control, and the ability to treat uncertainties characterized by time varying ideal weights. Conventional MRAC employs the assumption that the uncertainty must be characterized by a set of constant ideal weights, whereas with DF-MRAC the ideal weights can be time varying. This greatly reduces the burden on the designer in carefully selecting the correct set of basis functions in the design process. Another added advantage is that time delay parameter employed in DF-MRAC adds an additional degree of freedom that has the added advantage of introducing greater memory into the learning process.

Figures 12 and 13 illustrate how DF-MRAC is added an option to the ADMIRE simulation. To date it has be found that this option greatly improves the ability to handle failure in actuation. The ADMIRE aircraft is now able to restore its stabilization and maintain its desired mission performance for all the alternative CA methods that are currently implemented. This improved performance is illustrated in Figures 15-18 for the same case of stuck inboard elevons, previously shown in Figures 5-8 without adaptation. Figures 15a and 15b present the IFC's ability to maintain the aircraft controllability and restore stability when subjected to two stuck IB elevons and maintain a good command following under this degraded flight condition (Figure 15b.)

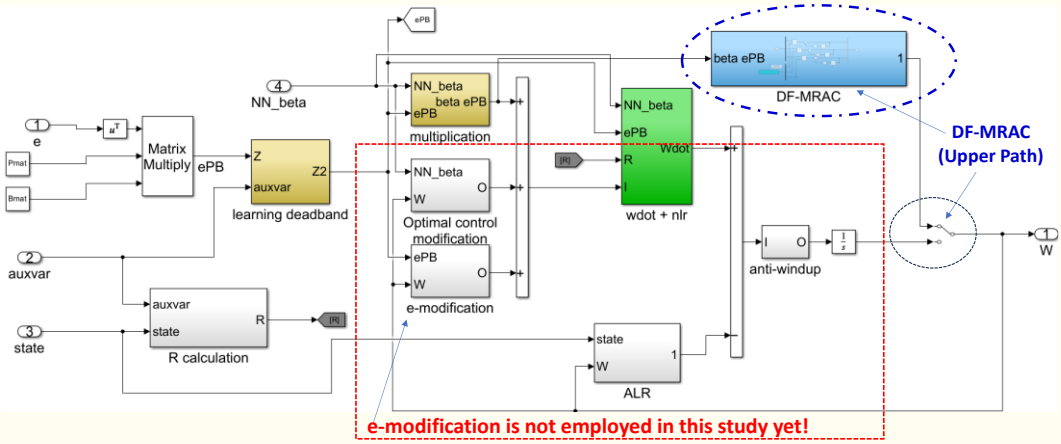

Figure 12: DF-MRAC Implementation in Parallel with Derivative Based MRAC

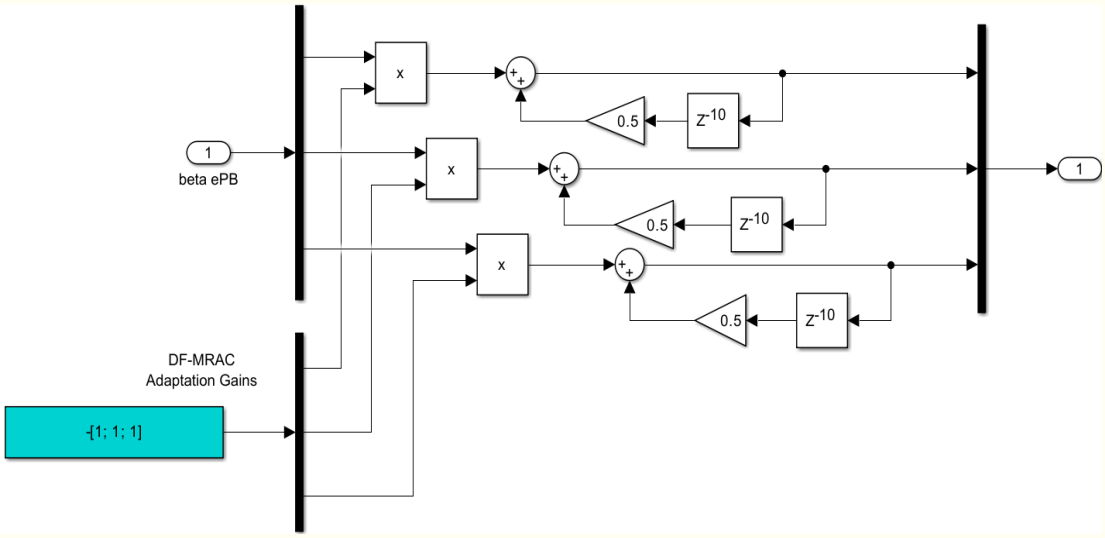

Figure 13: DF-MRAC Implementation within the IFC Architecture.

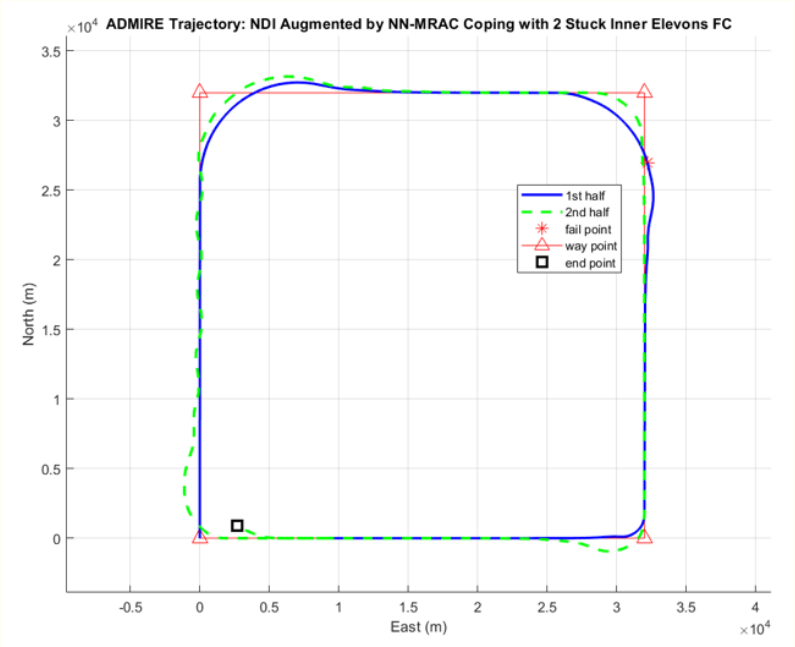

Figure 14: IFC/NDI Restoring Stabilization and Control Subject to Stuck Inboard Elevons Sufficient to Complete the Mission by Employing DF-MRAC.

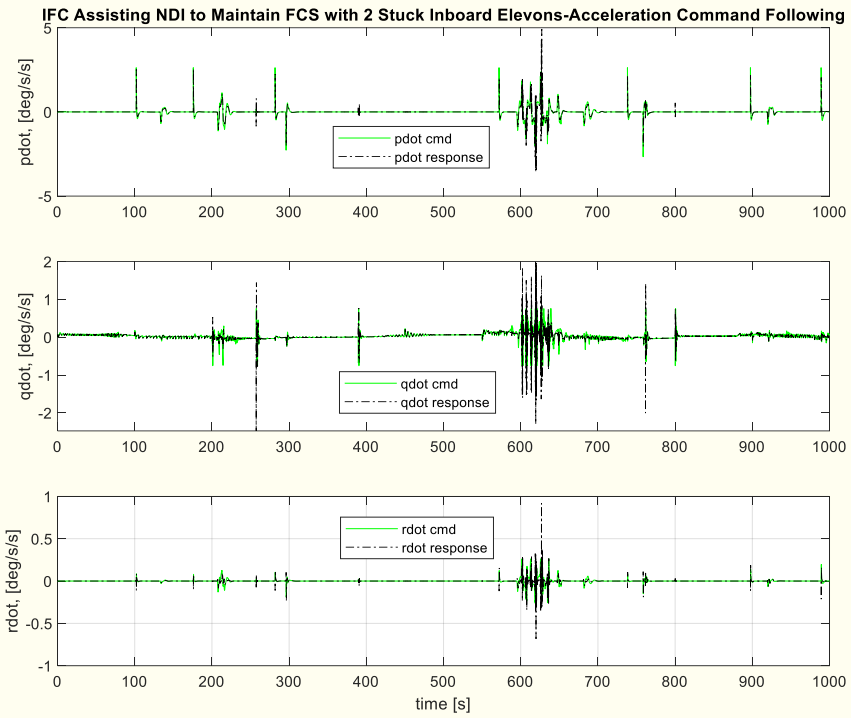

Figure 15a: Restored Stabilization by IFC with Improved Angular Acceleration Command Following Subject to 2 Stuck Inboard Elevons (see zoom-in region in Figure 15b for command following accuracy.)

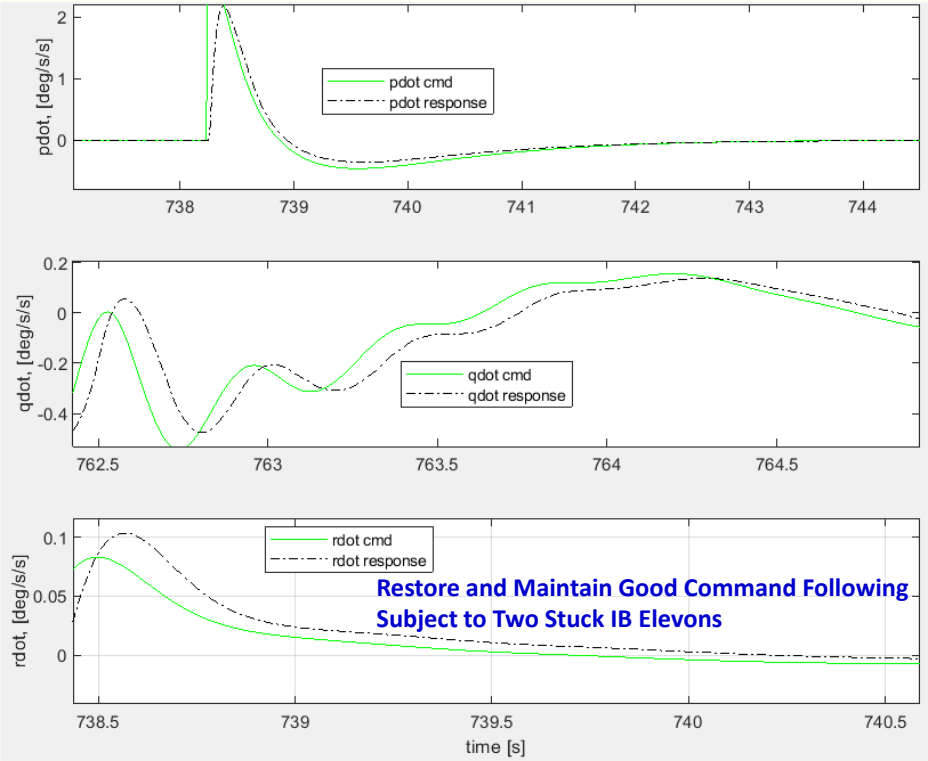

Figure 15b: Restored Stabilization by IFC with a zoom-in snapshot for command following restoration illustration (presented in the Figure 15a.)

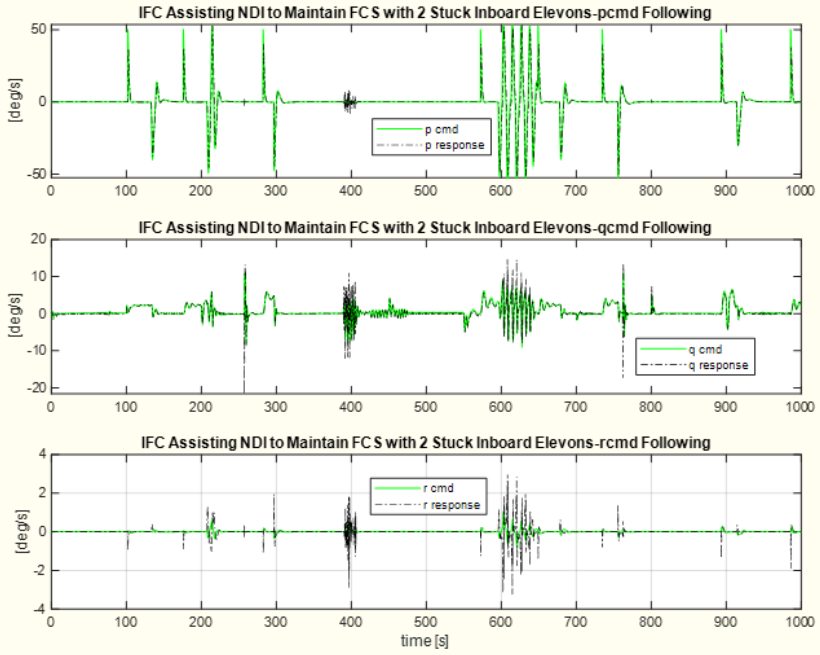

Figure 16: Restored Stabilization by IFC with Improved Angular Rate Command Following Subject to 2 Stuck Inboard Elevons.

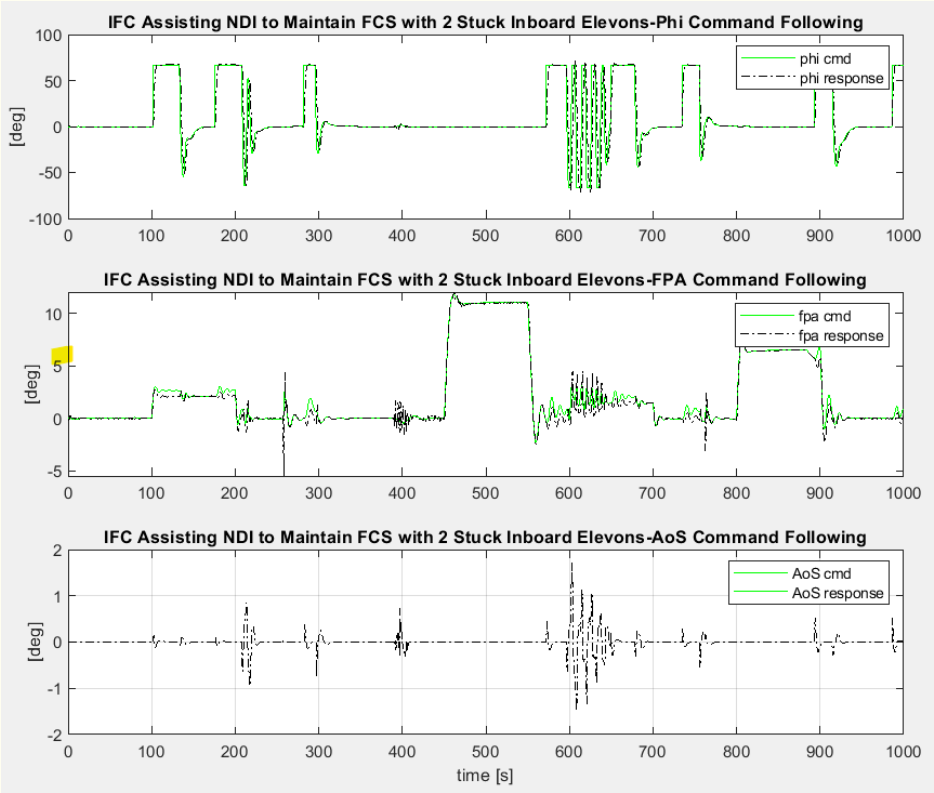

Figure 17: Restored Stabilization by IFC with Improved Angle Command Following and Tracking Subject to 2 Stuck Inboard Elevons.

5. IFC Extension with Direct Adaptive Control (DAC) Algorithm to CA Interaction

This section is a preliminary effort addressing F/M closed-loop regulation (i.e., enhancing F/M response to F/M commands generated by the inner loop NDI controller) which is the immediate layer tightly connected and interacting with the CA functional block presented in Figure 19. This is still being viewed as an adaptation protection layer which is implemented on the CLAW side (and not the CA side.) This is a part of the hybrid direct and indirect adaptive control design framework presented earlier in Figure 9.

The closest connection to CA in an adaptive sense (without explicitly solving the dynamic CA problem as described in [20-22]) is to actively regulate the angular acceleration error with some quadratic minimization adaptive regulator. We chose the direct adaptive control algorithm presented in [23] (and recently demonstrated in [10]) to actively enforce angular acceleration command following in the presence of degraded effectors. Surprisingly the use of such a direct adaptive control scheme as an adaptive acceleration error regulator works quite well for both stuck control surfaces and degraded effectors deflection angle and deflection rate limits (see Figure 18 for its adaptive gain real time adjusting as a function of model following errors of angular acceleration vector.)

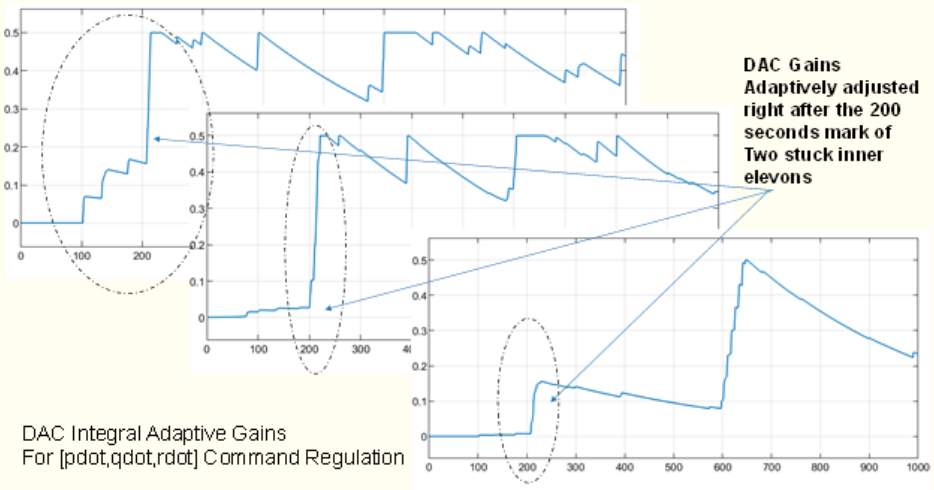

Figure 18: DAC Gain Adaptation Coping with Two Stuck IB Elevons

The CA design framework has been employed by the aircraft, UAVs, and spacecraft industries for more than 5 decades. However, various design algorithms and their design evolution are only captured by technical publications and internal technical memorandum until 2017 with a formal textbook by Durham, Bordignon, and Beck [6]. This textbook is viewed as a compilation of multi-decades research and development (R&D) in CA algorithms for aircraft FCS, especially with the mixing of NDI based design and the Cascaded Generalized Inverse (CGI) for X-35 and F-35 applications [7]. Readers are referred to Chapters 7 and 8 of the textbook [6] for the formal CA design framework captured therein and CA applications to the X-35 in Chapter 9. The concepts of ***Desired Commands*** (for Commanded Moments Generation by the inner loop NDI CLAW) vs ***Attenable Moments Set (AMS)*** via ***Admissible Control Effectors*** captured in the Appendix A of [6] and how they are being connected to the aircraft FCS design is captured in Appendix B. Note that the CA framework should be generalized for 6DOF control with full 6DOF F/M command following as described in Figure 18 below rather than solely moment or torque regulation.

The CA design framework interconnected to the CLAW side has been an active research topic during the last 10 years (e.g., see Innovative Control Effectors (ICE) [16] and balancing/resolving actuators redundancy via control vs control allocation [17]). It has become an important topic for maintaining high-speed UAV missions, especially under stressful operating conditions that include degraded effectors due to thermal impact or damages resulting from adversarial actions (see [18] and [19]).

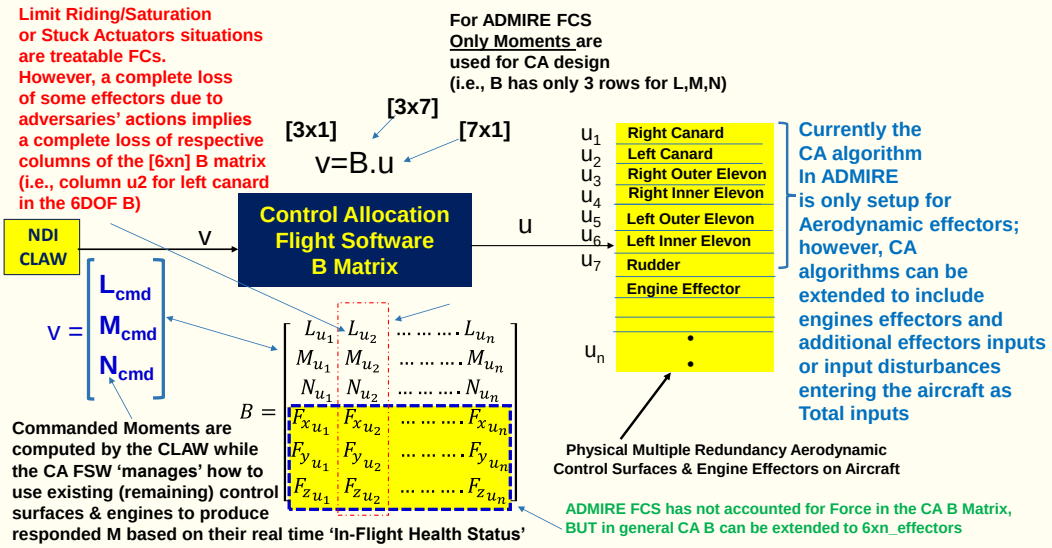

Figure 19: Full F/M Regulation with CA Framework Design Coupled with CLAW where 3DOF Force has been added to the baseline Moments.

The primary goal of adaptive CA dealing with control effectors failures is to dynamically reshape the CA multiple effectors blending matrix B (in Figure 18) to explicitly zero out the corresponding column of such a failed effector, so that the inner loop NDI CLAW does not rely on the same original number of healthy effectors for F/M contribution. In this example case, the control effector will be the 2nd column as illustrated in Figure 19. Therefore, the new B matrix used by the CLAW will now have a new dimension of [3x6] matrix (restructuring the B matrix by removing the 2nd column of its original [3x7] matrix) if the 2nd effector has been detected and declared as a complete loss of its operational capacity. Of course, other CA algorithms could offer effectors fault tolerant CA capabilities without explicitly restructuring the mixing matrix B such as in [24].

6. Concluding Remarks and Future Directions

The study presented herein, adaptive control augmentation via IFC to assist the primary baseline FCS subject to off-nominal FCs, is not new (e.g., see [4] and its cited references therein or [12] for a formality of adaptive control verification and validation.) We re-use such an attractive IFC solution for high-speed UAVs applications as an added extra layer of flight control protection exploiting its self-learning and adaptation consistency. One important finding is that the IFC DF-MRAC works very well with all existing 7 CA algorithms to maintain FCS performance while the DAC algorithms are only operational to 3 of them using the same set of adaptation parameters selection. This means the DAC algorithm requires retuning of its adaptation parameters ($[\Gamma_I,\Gamma_p,\sigma]$, see [23]) for different CA algorithms while the IFC algorithms do not require retuning. The current IFC design will be continuously evaluated, revised, and upgraded to address more formal failure cases and to mature its design to serve more realistic high speed UAVs missions.

Future directions will extend the IFC design to address the functional CA performance aspects (augmentation of the CA functional blocks subject to effectors performance degradation, e.g., see [18-22] or [24]) rather than just adaptation augmentation added on in the control law side of the FCS. As mentioned earlier in Section 5, there are two main paths (e.g., see [17]) to dynamically size/shape and determine the commanded effectors: (1) directly determine the real deflection of effectors from the applied optimal control and (2) use optimal control or NDI to compute the total F/M, and then use the actual CA function (via the multiple effectors mixing matrix B in Figure 19) to compute individual effectors' deflection in real time. Aircraft CA algorithms have been extensively studied during the past two decades (e.g., see [6] and references cited therein) and are still considered an active research area in addressing CA mixing to achieve (i) optimal performance when all effectors are healthy and (ii) suboptimal performance when effectors are in degraded operating conditions (e.g., see [33] for actively reshaping the effectors blender solution B matrix in real time (see Figure 4 of [33])) while still able to maintain the designated mission.

There are future improvements contemplated for IFC in general and DF-MRAC in particular. These include:

a) Adaptive Hedging to improve response when actuator position and rate limits are active and to account for the fact that actuators are bandwidth limited (see [25]).

b) Adaptive Loop Transfer Recovery to guarantee the gain, phase and time delay margins of the baseline design are preserved under IFC (see [26])

c) A direct method for adaptation to actuator failures that does not require augmentation of the CA function blocs. This involves a modification to Eq. (12) as described in section 3.4 of [9].

d) Application of a neural network-based control to attenuate external disturbances developed by Levin and Ioannu in [27]

e) Possibility of employing the multiple model adaptive mixing schemes developed in [28] and [29] to ensure a wider region of adaptation without model switching.

Acknowledgments

This study is part of a bigger campaign in preparation for future high speed UAVs business pursuit and partially was funded by the Jesplsoft IRAD Program. The NASA partnership forming and support are greatly appreciated.

Conflict of Interest

"The authors declare no conflict of interest."

References

[1] N. Eva Wu, “Reliability Analysis for AFTI-F16 SRFCS Using ASSIST and SURE,” Proceedings of the American Control Conference Anchorage, AK May 8-1 0,2002
[2] Rudaba Khan , Paul Williams , Paul Riseborough , Asha Rao , and Robin Hill, “Active Fault Tolerant Flight Control System Design - A UAV Case Study,” arXiv:1610.03162v1, 2016
[3] B. Hu, P. Seiler, “A Probabilistic Method For Certification of Analytically Redundant Systems,” IEEE 2013
[4] Nhan Nguyen, Kalmanje Krishnakumar, John Kaneshige, Pascal Nespeca, "Flight Dynamics and Hybrid Adaptive Control of Damaged Aircraft," JOURNAL OF GUIDANCE, CONTROL, AND DYNAMICS, Vol. 31, No. 3, May–June 2008
[5] Lars Forssell and Ulrik Nilsson, “ADMIRE The Aero Data Model in Research Environment Version 4, Model Description”, Report No. FOI-R--1624--SE, FOI Swedish Defense Research Agency, Systems Technology, SE -164 90, Stockholm, 2005
[6] W. Durham, K. Bordignon, and R. Beck, **Aircraft Control Allocation**, Wiley Aerospace Series, 2017
[7] Bordignon, K and Bessolo, J. ‘Control allocation for the X-35B,’ AIAA 2002-6020 in 2002 Biennial International Powered Lift Conference and Exhibit, 5-7 November 2002, Williamsburg, Virginia
[8] P Lathasree, Abhay A Pashilkar and N Sundararajan, “Application of Generic Flight Controller Design Approach for A Delta Canard Fighter Aircraft -ADMIRE,” 2019 Sixth Indian Control Conference (ICC) December 18-20, 2019. IIT Hyderabad, India
[9] T. Yucelen and A. J. Calise, **Derivative-Free Adaptive Control**, AIAA Volume 267, 2023
[10] Q. Lam, "Direct Adaptive Control Augmentation and Dynamic Control Allocation Algorithms Subject to Stuck Control Elevons for Aircraft Flight Control Robustness and Performance Enhancement," Jesplsoft IRAD Report August 2023, https://Jesplsoft.com
[11] Xingsheng Li, Shiyue Liu, Fuhui Guo, Sihua Zhang, “Fault-Tolerant Control Based on Control Allocation for Hypersonic Vehicle with Actuator Stuck Fault,” IEEE 2019
[12] Nhan Nguyen, “Verification and Validation Challenges for Adaptive Flight Control of Complex Autonomous Systems,” AIAA 2018
[13] Rysdyk, R. T., and Calise, A. J., “Fault Tolerant Flight Control via Adaptive Neural Network Augmentation,” AIAA Guidance, Navigation, and Control Conference, AIAA 1998-4483, 1998
[14] Narendra, K. S., and Annaswamy, A. M., “New Adaptive Law for Robust Adaptation Without Persistent Excitation,” IEEE Transactions on Automatic Control, Vol. 32, No. 2, 1987, pp. 134–145
[15] A. J. Calise, M. Sharma, and J. E. Corban, “Adaptive Autopilot Design for Guided Munitions,” Journal of G&C Dynamics Sept-Oct 2000
[16] Niestroy, M.A, Dorsett, K.M., and Markstein, K., “A Tailless Fighter Aircraft Model for Control-Related Research and Development,” AIAA 2016
[17] Ola Harkega_ard, Torkel Glad, “Resolving actuator redundancy: Optimal control vs. control allocation,” 2004, (see http://www.control.isy.liu.se)
[18] Yong FAN, Ji-hong ZHU, Jia-qiang ZHU and Zeng-qi SUN, “Genetic Algorithm Based Constrained Control Allocation for Tailless Fighter,” the National High Technology Research and Development Program of China Grant #2005AA751010

[19] Ling-yu Yang, You-wu Zhong, Gong-zhang Shen, “Control Allocation and Management for Aircraft with Multiple Effectors,” IEEE 2009
[20] B. Lu, J. Ma, and Z. Zheng, “Adaptive Closed-Loop Control Allocation Based Fault Tolerant Flight Control for an Over-Actuated Aircraft,” IEEE 2019
[21] Shi Jingping, Lv Yongxi, Qu Xiaobo, and Shi Jing, “A Coordinated Control Method of Thrust Vector and Aerodynamic Surfaces Based on Control Allocation Technology,” IEEE 2018
[22] Lei Cui, Zhiqiang Zuo , and Ying Yang, “A Control-Theoretic Study on Iterative Solution to Control Allocation for Over-Actuated Aircraft, IEEE 2018
[23] Q. Lam & I. Barkana, “Direct Adaptive Control Treatment to Flight Control Input Saturation,” AIAA 2005
[24] M. T. Hamayun, C. Edwards, H. Alwi, A. Bajodah, “A Fault Tolerant Direct Control Allocation Scheme With Integral Sliding Modes,” Int. J. Appl. Math. Comput. Sci., 2015, Vol. 25, No. 1, 93–10
[25] Johnson, E.N., Calise, A., “Limited Authority Adaptive Flight Control for Reusable Launch Vehicles,” Journal of Guidance, Control and Dynamics, Vol. 26, No. 6, Nov-Dec. 2003, pp. 926-913
[26] Calise, A.J., Yucelen, T., “Adaptive Loop Transfer Recovery,” AIAA Journal of Guidance, Control, and Dynamics, Vol. 35, No. 3, May-June 2012, pp. 807-815.
[27] Jason Levin and Petros A. Ioannu, “Adaptive Control with Neuro-Adaptive Disturbance Rejection,” 17th Mediterranean Conference on Control & Automation Makedonia Palace, Thessaloniki, Greece, 2009
[28] Matthew Kuipers, Petros Ioannou, Barıs¸ Fidan, and Maj Mirmirani, “Analysis of an Adaptive Mixing Control Scheme for an Airbreathing Hypersonic Vehicle Model,” 2009 American Control Conference Hyatt Regency Riverfront, St. Louis, MO, USA June 10-12, 2009
[29] Q. Lam, J. Cloutier, A. Hart, and S. Stockbridge, “Exploring Multiple Model Control Mixing for Robustness and Performance Enhancement of Hypersonic Vehicles,” Proceedings of the Joint Army Navy-NASA-Air Force Conference, December 2014
[30] Nguyen, N., *Model-Reference Adaptive Control - a Primer*, Springer-Verlag, ISBN 3319563920, March 2018.
[31] Campbell, S., Kaneshige, J., Nguyen, N., and Krishnakumar, K., “An Adaptive Control Simulation Study Using Pilot Handling Qualities Evaluations,” AIAA Guidance, Navigation, and Control Conference, AIAA-2010-8013, August 2010.
[32] Nguyen, N., Hanson, C., Burken, J., and Schaefer, J., “Normalized Optimal Control Modification and Flight Experiments on NASA F/A-18 Aircraft,” AIAA Journal of Guidance, Control, and Dynamics, Vol. 40, pp. 1061-1075, April 2017.
[33] Jeffrey J Harris and James Richard Stanford, “F-35 Flight Control Law Design, Development, and Verification,” AIAA Aviation Forum, 2018